

Effect of dephasing on transient and steady-state entanglement in a quantum-beat laser

Eyob A. Sete*

Institute for Quantum Science and Engineering and Department of Physics and Astronomy, Texas A&M University, College Station, Texas 77843-4242, USA

(Received 10 September 2011; published 5 December 2011)

We study the role of dephasing on entanglement evolution in a two-photon quantum-beat laser. We rigorously derived the pertinent master equation by taking into account dephasing, spontaneous emission, and cavity losses. The dephasing rate, in general, is larger than the rates of other dissipation processes and might influence the realizable quantum properties of the cavity field. We investigate the extent to which the dephasing rate affects the transient as well as steady-state entanglement between the cavity modes. We show that the coherence induced by initial coherent superposition of atomic levels leads to transient as well as steady-state entanglement, which turns out to be susceptible to decoherence. However, the entanglement created via coherence induced by a strong laser field exists for only short times and is relatively robust against decoherence.

DOI: [10.1103/PhysRevA.84.063808](https://doi.org/10.1103/PhysRevA.84.063808)

PACS number(s): 42.50.Ct, 03.67.Bg, 42.50.Nn

I. INTRODUCTION

Quantum properties of cavity radiation strongly rely on the dissipation processes that the system is subjected to. Among all dissipation processes, dephasing—the decay of atomic coherence due to its interaction with the surrounding environment—might lead to adverse effects on the quantum features of the cavity field. In particular, quantum entanglement is fragile in the face of decoherence. Recently, entanglement generation using two-photon lasers such as correlated emission lasers [1–3] and quantum-beat lasers (QBLs) [4–7] has received renewed interest. In these types of lasers, the entanglement is dependent on quantum coherence and is susceptible to dephasing processes. Here we address the role of dephasing on entanglement generated by quantum-beat lasers.

The quantum-beat laser concept was originally used as a means of quenching of spontaneous emission noise [8–12] and later for demonstration of lasing without population inversion [13]. Recently, QBLs have also been proposed as a source of entangled radiation [4–7]. In such lasers, the generated entanglement is attributed to atomic coherence induced via coupling the upper two levels of V-type three-level atoms by a strong laser field or *driven coherence*. This coherence translates into correlations between two modes of the cavity field due to interference between the two pathways that lead to the lower level. Note that since the generated coherence crucially depends on the amplitude of the laser field [4–6], the time for which the cavity exhibits entanglement strongly relies on the strength of the driving field. It has also been shown that the entanglement created via driven coherence only exists in the transient regime and hence depends on the initial condition of the cavity field. Besides, all previous studies of QBLs neglected dephasing processes which otherwise lead to fast decay of coherence and hence entanglement. For a practical application of quantum information processing, it is desirable to have entanglement which can survive for longer times and is robust against decoherence.

This work is thus devoted to the formulation and analysis of the role of dephasing on entanglement properties of the cavity modes of a QBL. We present a detailed derivation of the pertinent master equation in the good cavity limit by taking into account all dissipation processes, namely spontaneous emission, cavity losses, and dephasing. Unlike earlier studies where driven coherence is used as a primary way of inducing coherence in the system, our scheme includes coherence induced via initial coherent superposition of the two upper levels of V-type atoms or *injected coherence*. We investigate to what extent the dephasing rate modifies the entanglement between the cavity modes for the cases of injected coherence as well as driven coherence using the Hillery-Zubairy (HZ) entanglement criterion [14]. We also discuss the interplay between the cavity mode detunings and pumping rates in optimizing the entanglement. Our results show that when the coherence is induced by initial coherent superposition of atomic levels, the resulting entanglement exists both in transient as well as steady-state regimes and is more sensitive to dephasing processes. In particular, the steady-state entanglement is achieved when only cavity mode detunings are different. We also show that it is possible to reduce the effect of dephasing on entanglement by injecting atoms at higher rates and tuning the cavity modes at far-off resonances (large detunings). In contrast, when coherence is induced by coupling the upper two levels with a strong laser field, we obtain only transient entanglement, which is relatively robust against decoherence.

II. HAMILTONIAN AND MASTER EQUATION

We consider a two-photon QBL coupled to a vacuum reservoir through the partially transmitting mirror of the cavity. Atoms, in the so-called V configuration, are injected into the laser cavity at rate r_a and are removed after time τ longer than the spontaneous emission time. During this time interval, each atom nonresonantly interacts with the cavity modes of frequencies ν_1 and ν_2 . Moreover, to externally induce coherence, a strong laser field of Rabi frequency Ω and phase ϕ is resonantly coupled to the $|a_1\rangle \leftrightarrow |a_2\rangle$ transition. The energy level diagram for the atom is shown in Fig. 1. The

*eyobas@physics.tamu.edu

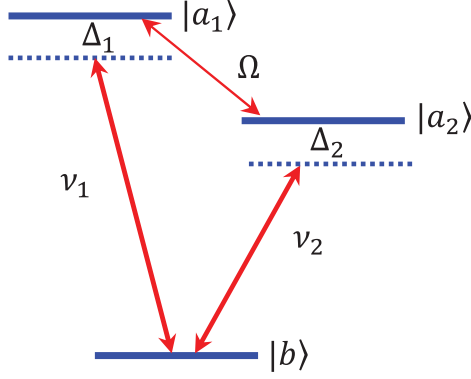


FIG. 1. (Color online) Energy level diagram for a three-level atom in a V configuration.

interaction picture Hamiltonian for the system, in the rotating wave and dipole approximations, is given by ($\hbar = 1$)

$$\hat{H}_I = \sum_{j=1}^2 \Delta_j |a_j\rangle \langle a_j| + g_j (\hat{a}_j |a_j\rangle \langle b| + |b\rangle \langle a_j| \hat{a}_j^\dagger) - \frac{\Omega}{2} (e^{-i\phi} |a_1\rangle \langle a_2| + e^{i\phi} |a_2\rangle \langle a_1|). \quad (1)$$

Here \hat{a}_1 (\hat{a}_1^\dagger) and \hat{a}_2 (\hat{a}_2^\dagger) are the annihilation (creation) operators for the cavity modes 1 and 2, respectively, and g_i are atom-cavity mode coupling constants. The modes of the cavity are detuned from the transitions $|a_1\rangle \leftrightarrow |b\rangle$ and $|a_2\rangle \leftrightarrow |b\rangle$ by $\Delta_1 = \omega_{1b} - \nu_1$ and $\Delta_2 = \omega_{2b} - \nu_2$, respectively.

We next derive the master equation for the cavity radiation by applying the Hamiltonian (1). While there are several approaches for obtaining the master equation, we here employ the procedure outlined in [15–17]. Suppose that $\hat{\rho}_{AR}(t, t_j)$ represent the density operator for the radiation plus an atom in the cavity at time t that is injected at earlier time t_j . Since the atom stays in the cavity for time τ , it easy to see that $t - \tau \leq t_j \leq t$. Then the density operator for all atoms in the cavity plus the two-mode radiation at time t can be written as

$$\hat{\rho}_{AR}(t) = r_a \sum_j \hat{\rho}_{AR}(t, t_j) \Delta t'_j, \quad (2)$$

where $r_a \Delta t'_j$ is the total number of atoms injected into the cavity in a small time interval $\Delta t'_j$. Assuming that large number of atoms are injected in time interval Δt_j , we can change the summation by integration. Thus differentiating both sides of the resulting equation, we arrive at

$$\frac{d}{dt} \hat{\rho}_{AR}(t) = r_a \frac{d}{dt} \int_{t-\tau}^t \hat{\rho}_{AR}(t, t') dt'. \quad (3)$$

In order to incorporate the initial preparation of the atoms into the dynamics, we transform the above equation using a useful mathematical identity to [18]

$$\begin{aligned} \frac{d}{dt} \hat{\rho}_{AR}(t) &= r_a \left\{ [\hat{\rho}_{AR}(t, t) - \hat{\rho}_{AR}(t, t - \tau)] + \int_{t-\tau}^t \frac{\partial}{\partial t} \hat{\rho}_{AR}(t, t') dt' \right\}. \end{aligned} \quad (4)$$

Here $\hat{\rho}_{AR}(t, t)$ represents the density operator for atom plus radiation at time t for an atom injected at an earlier time t . Since the atomic and radiation variables are uncorrelated at the instant the atom is injected into the cavity, one can write

$$\hat{\rho}_{AR}(t, t) \equiv \hat{\rho}(t) \hat{\rho}_A(0), \quad (5)$$

where $\hat{\rho}(t)$ is the cavity radiation density operator and $\hat{\rho}_A(0)$ is the initial density operator for an atom. For simplicity, we further assume that the atomic and radiation variables are uncorrelated just after the atom is removed from the cavity, which allows us to write

$$\hat{\rho}_{AR}(t, t - \tau) \equiv \hat{\rho}(t) \hat{\rho}_A(t - \tau), \quad (6)$$

where $\hat{\rho}_A(t - \tau)$ is the density operator for an atom injected at $t - \tau$. In this work, we assume that atoms are initially injected into the cavity in coherent superposition of the upper two levels. The corresponding initial density operator then reads

$$\begin{aligned} \hat{\rho}_A(0) &= \rho_{11}^{(0)} |a_1\rangle \langle a_1| + \rho_{22}^{(0)} |a_2\rangle \langle a_2| + \rho_{12}^{(0)} |a_1\rangle \langle a_2| \\ &+ \rho_{21}^{(0)} |a_2\rangle \langle a_1|, \end{aligned} \quad (7)$$

where $\rho_{ii}^{(0)}$ and $\rho_{ij}^{(0)}$ are initial population and coherence, respectively. Using Eqs. (5), (6), and (4) becomes

$$\begin{aligned} \frac{d}{dt} \hat{\rho}_{AR}(t) &= r_a \left\{ [\hat{\rho}_A(0) - \hat{\rho}_A(t - \tau)] \hat{\rho} + \int_{t-\tau}^t \frac{\partial}{\partial t} \hat{\rho}_{AR}(t, t') dt' \right\}. \end{aligned} \quad (8)$$

Furthermore, it is obvious that the time evolution of the density operator $\hat{\rho}_{AR}(t, t')$ has a form $\partial \hat{\rho}_{AR}(t, t') / \partial t = -i[H_I, \hat{\rho}_{AR}(t, t')]$ which together with $\partial \hat{\rho}_{AR}(t) / \partial t = r_a \int_{t-\tau}^t (\partial \hat{\rho}_{AR}(t, t') / \partial t) dt'$ leads to

$$\frac{d}{dt} \hat{\rho}_{AR}(t) = r_a [\hat{\rho}_A(0) - \hat{\rho}_A(t - \tau)] \hat{\rho} - i[H_I, \hat{\rho}_{AR}(t)]. \quad (9)$$

We are interested in the dynamics of the cavity radiation. In this regard, we trace the atom plus radiation density operator over atomic variables. This yields

$$\frac{d}{dt} \hat{\rho}(t) = -i \text{Tr}_A [H_I, \hat{\rho}_{AR}(t)], \quad (10)$$

where we have used the fact that $\text{Tr}_A [\hat{\rho}_A(0)] = \text{Tr}_A [\hat{\rho}_A(t - \tau)] = 1$. By substituting the Hamiltonian in Eq. (10) we obtain

$$\begin{aligned} \frac{d}{dt} \hat{\rho}(t) &= -i g_1 (a_1 \hat{\rho}_{b1} - \hat{\rho}_{b1} a_1 + a_1^\dagger \hat{\rho}_{1b} - \hat{\rho}_{1b} a_1^\dagger) \\ &- i g_2 (\hat{a}_2 \hat{\rho}_{b2} - \hat{\rho}_{b2} \hat{a}_2 + \hat{a}_2^\dagger \hat{\rho}_{2b} - \hat{\rho}_{2b} \hat{a}_2^\dagger). \end{aligned} \quad (11)$$

The next task is to obtain $\hat{\rho}_{b1}$, $\hat{\rho}_{b2}$ and their complex conjugates. To this end, by multiplying Eq. (9) on the left by $\langle \alpha|$ and on the right by $|\beta\rangle$ one gets

$$\begin{aligned} \frac{d}{dt} \hat{\rho}_{\alpha\beta}(t) &= r_a \langle \alpha| [\hat{\rho}_A(0) - \hat{\rho}_A(t, t - \tau)] |\beta\rangle \hat{\rho} \\ &- i \langle \alpha| [H_I, \hat{\rho}_{AR}(t)] |\beta\rangle - \gamma_{\alpha\beta} \hat{\rho}_{\alpha\beta}, \end{aligned} \quad (12)$$

where $\alpha, \beta = a_1, a_2, b$. We phenomenologically included the last term to account for spontaneous emission and dephasing processes. $\gamma_{\alpha\alpha}$ is the spontaneous emission rate, and $\gamma_{\alpha\beta}$ ($\alpha \neq \beta$) is the dephasing rate. The equations of motion

for the elements of the density operator that appear in Eq. (11) read

$$\begin{aligned} \dot{\hat{\rho}}_{1b} = & -(\Gamma_1 + i\Delta_1)\hat{\rho}_{1b} + ig_1(\hat{\rho}_{11}\hat{a}_1 - \hat{a}_1\hat{\rho}_{bb}) \\ & + ig_2\hat{\rho}_{12}\hat{a}_2 + \frac{i\Omega}{2}e^{-i\phi}\hat{\rho}_{2b}, \end{aligned} \quad (13)$$

$$\begin{aligned} \dot{\hat{\rho}}_{2b} = & -(\Gamma_2 + i\Delta_2)\hat{\rho}_{2b} + ig_2(\hat{\rho}_{22}\hat{a}_2 - \hat{a}_2\hat{\rho}_{bb}) \\ & + ig_1\hat{\rho}_{21}\hat{a}_1 + \frac{i\Omega}{2}e^{i\phi}\hat{\rho}_{2b}. \end{aligned} \quad (14)$$

Here Γ_1 and Γ_2 are the dephasing rates for single-photon coherence terms $\hat{\rho}_{1b}$ and $\hat{\rho}_{2b}$, respectively.

To proceed further, we adopt certain approximation schemes. The first is the good cavity limit where the cavity damping rate is much smaller than the dephasing and spontaneous emission rates. In this limit, the cavity mode variables vary more slowly than the atomic variables, and thus the atomic variables reach steady state in a short time. The time derivatives of such variables can be set to zero, keeping the cavity mode variables at time t , which is also called *adiabatic approximation*. Moreover, we apply a linearization scheme which amounts to retaining terms up to second order in the cavity-atom coupling constant g in the master equation. To do so, we first write the equations of motion for $\hat{\rho}_{11}$, $\hat{\rho}_{22}$, $\hat{\rho}_{12}$, and $\hat{\rho}_{bb}$ in the zero order in the coupling constant:

$$\dot{\hat{\rho}}_{11} = r_a\rho_{11}^{(0)}\hat{\rho} + \frac{i\Omega}{2}(\exp^{-i\phi}\hat{\rho}_{21} - e^{i\phi}\hat{\rho}_{12}) - \gamma_1\hat{\rho}_{11}, \quad (15)$$

$$\dot{\hat{\rho}}_{22} = r_a\rho_{22}^{(0)}\hat{\rho} + \frac{i\Omega}{2}(\exp^{i\phi}\hat{\rho}_{12} - e^{-i\phi}\hat{\rho}_{21}) - \gamma_2\hat{\rho}_{22}, \quad (16)$$

$$\dot{\hat{\rho}}_{12} = r_a\rho_{12}^{(0)}\hat{\rho} + \frac{i\Omega}{2}\exp^{-i\phi}(\hat{\rho}_{22} - \hat{\rho}_{11}) - \Gamma_{12}\hat{\rho}_{12}, \quad (17)$$

$$\dot{\hat{\rho}}_{bb} = 0, \quad (18)$$

in which γ_1 and γ_2 are spontaneous emission rates of levels $|a_1\rangle$ and $|a_2\rangle$ to lower level $|b\rangle$, respectively; Γ_{12} is the two-photon dephasing rate. Now we apply the adiabatic approximation, that is, set the time derivatives in Eqs. (15)–(17) to zero to obtain

$$\hat{\rho}_{11} = \frac{r_a\hat{\rho}}{\chi}[\gamma_2(1-\eta)\Gamma_{12} + \Omega^2 + \gamma_2\Omega\sqrt{1-\eta^2}\sin\phi], \quad (19)$$

$$\hat{\rho}_{22} = \frac{r_a\hat{\rho}}{\chi}[\gamma_1(1+\eta)\Gamma_{12} + \Omega^2 - \gamma_1\Omega\sqrt{1-\eta^2}\sin\phi], \quad (20)$$

$$\begin{aligned} \hat{\rho}_{12} = & \frac{r_a\hat{\rho}}{2\Gamma_{12}\chi}\{\sqrt{1-\eta^2}(\chi\cos\phi - 2i\Gamma_{12}\gamma_1\gamma_2\sin\phi) \\ & + i\Gamma_{12}[\gamma_1 - \gamma_2 + (\gamma_1 + \gamma_2)\eta]\Omega\}e^{-i\phi}, \end{aligned} \quad (21)$$

where $\chi = 2\gamma_1\gamma_2\Gamma_{12} + (\gamma_1 + \gamma_2)\Omega^2$. Here we have introduced a useful notation where $\rho_{11}^{(0)} = (1-\eta)/2$, $\rho_{22}^{(0)} = (1+\eta)/2$, and $\rho_{12}^{(0)} = \frac{1}{2}\sqrt{1-\eta^2}$. It is easy to see that $\rho_{12}^{(0)} = [0, \frac{1}{2}]$, with 0 being no coherence and $\frac{1}{2}$ corresponds to maximum coherence. In Sec. III A, we will show that this coherence is responsible for the entanglement of the cavity modes. By applying the adiabatic approximation in Eqs. (13) and (14) and using the solutions for $\hat{\rho}_{11}$, $\hat{\rho}_{22}$, $\hat{\rho}_{12}$, we obtain

$$-ig_1\hat{\rho}_{1b} = \zeta_{11}\hat{\rho}\hat{a}_1 + \zeta_{12}\hat{\rho}\hat{a}_2, \quad (22)$$

$$-ig_2\hat{\rho}_{2b} = \zeta_{22}\hat{\rho}\hat{a}_2 + \zeta_{21}\hat{\rho}\hat{a}_1. \quad (23)$$

Explicit expressions for the coefficients ζ_{ij} ($i = 1, 2$) are given in Appendix A. Therefore, using Eqs. (22), (23), and (11) and taking into account the damping of cavity modes by vacuum reservoir, the master equation for the cavity radiation becomes

$$\begin{aligned} \dot{\hat{\rho}} = & \zeta_{11}^*(\hat{a}_1^\dagger\hat{\rho}\hat{a}_1 - \hat{a}_1\hat{a}_1^\dagger\hat{\rho}) + \zeta_{11}(\hat{a}_1^\dagger\hat{\rho}\hat{a}_1 - \hat{\rho}\hat{a}_1\hat{a}_1^\dagger) \\ & + \zeta_{22}^*(\hat{a}_2^\dagger\hat{\rho}\hat{a}_2 - \hat{a}_2\hat{a}_2^\dagger\hat{\rho}) + \zeta_{22}(\hat{a}_2^\dagger\hat{\rho}\hat{a}_2 - \hat{\rho}\hat{a}_2\hat{a}_2^\dagger) \\ & + [\zeta_{21}^*(\hat{a}_1^\dagger\hat{\rho}\hat{a}_2 - \hat{a}_1\hat{a}_2^\dagger\hat{\rho}) + \zeta_{12}(\hat{a}_1^\dagger\hat{\rho}\hat{a}_2 - \hat{\rho}\hat{a}_1\hat{a}_2^\dagger)]e^{-i\phi} \\ & + [\zeta_{12}^*(\hat{a}_2^\dagger\hat{\rho}\hat{a}_1 - \hat{a}_2\hat{a}_1^\dagger\hat{\rho}) + \zeta_{21}(\hat{a}_2^\dagger\hat{\rho}\hat{a}_1 - \hat{\rho}\hat{a}_2\hat{a}_1^\dagger)]e^{i\phi} \\ & + \sum_{j=1}^2 \frac{\kappa_j}{2}(2\hat{a}_j\hat{\rho}\hat{a}_j^\dagger - \hat{a}_j^\dagger\hat{a}_j\hat{\rho} - \hat{\rho}\hat{a}_j^\dagger\hat{a}_j), \end{aligned} \quad (24)$$

where κ_j is the damping rate of the j th cavity mode. The terms proportional to ζ_{11} and ζ_{22} represent gain for cavity modes 1 and 2, respectively, whereas terms proportional to ζ_{12} and ζ_{21}^* are phase sensitive and are due to atomic coherence.

III. ENTANGLEMENT OF CAVITY MODES

Here we analyze the behavior of entanglement of the cavity field when the coherence is induced by initial coherent superposition of atoms. In general, criteria proposed to detect bipartite entanglement rely on the nature of the field, field Gaussianity, and the form of the entanglement created. For instance, in a three-level QBL, since there are two possible pathways for an atom in coherent superposition of the upper two levels to decay to the lower level $|b\rangle$ the form of entanglement expected in our system is $\alpha|0_11_2\rangle + \beta|1_10_2\rangle$. Such type of entanglement can be detected by only a certain class of inseparability criteria [14,19,20]. In order to study the behavior of entanglement between the cavity modes, we employ the HZ entanglement criterion [14], which is sufficient to test for two-mode non-Gaussian states. This criterion relies on a combination of second- and fourth-order correlations among the cavity mode variables. According to this criterion, the two modes are entangled if the following inequality is satisfied:

$$E_{HZ} \equiv \langle \hat{n}_1\hat{n}_2 \rangle - |\langle \hat{a}_1^\dagger\hat{a}_2 \rangle|^2 < 0, \quad (25)$$

where $\hat{n}_1 = \hat{a}_1^\dagger\hat{a}_1$ and $\hat{n}_2 = \hat{a}_2^\dagger\hat{a}_2$ are photon number operators for the cavity modes.

A. Entanglement via injected coherence

In order to clearly see the contribution of the injected coherence in creating entanglement between the cavity modes, we turn off the driving field ($\Omega = 0$). The master equation corresponding to the injected coherence obtained by setting $\Omega = 0$ in the coefficients ζ_{ij} ($i, j = 1, 2$) in Eq. (24) reads

$$\begin{aligned} \dot{\hat{\rho}} = & \alpha_{11}^*(\hat{a}_1^\dagger\hat{\rho}\hat{a}_1 - \hat{a}_1\hat{a}_1^\dagger\hat{\rho}) + \alpha_{11}(\hat{a}_1^\dagger\hat{\rho}\hat{a}_1 - \hat{\rho}\hat{a}_1\hat{a}_1^\dagger) \\ & + \alpha_{22}^*(\hat{a}_2^\dagger\hat{\rho}\hat{a}_2 - \hat{a}_2\hat{a}_2^\dagger\hat{\rho}) + \alpha_{22}(\hat{a}_2^\dagger\hat{\rho}\hat{a}_2 - \hat{\rho}\hat{a}_2\hat{a}_2^\dagger) \\ & + [\alpha_{21}^*(\hat{a}_1^\dagger\hat{\rho}\hat{a}_2 - \hat{a}_1\hat{a}_2^\dagger\hat{\rho}) + \alpha_{12}(\hat{a}_1^\dagger\hat{\rho}\hat{a}_2 - \hat{\rho}\hat{a}_1\hat{a}_2^\dagger)]e^{-i\phi} \\ & + [\alpha_{12}^*(\hat{a}_2^\dagger\hat{\rho}\hat{a}_1 - \hat{a}_2\hat{a}_1^\dagger\hat{\rho}) + \alpha_{21}(\hat{a}_2^\dagger\hat{\rho}\hat{a}_1 - \hat{\rho}\hat{a}_2\hat{a}_1^\dagger)]e^{i\phi} \\ & + \sum_{j=1}^2 \frac{\kappa_j}{2}(2\hat{a}_j\hat{\rho}\hat{a}_j^\dagger - \hat{a}_j^\dagger\hat{a}_j\hat{\rho} - \hat{\rho}\hat{a}_j^\dagger\hat{a}_j), \end{aligned} \quad (26)$$

where

$$\alpha_{11} = \frac{g_1^2 r_a \Gamma_{12} \gamma_2 (1 + \eta)}{(\Gamma_1 + i \Delta_1) \chi}, \quad (27)$$

$$\alpha_{12} = \frac{g_1 g_2 r_a \sqrt{1 - \eta^2} (\chi \cos \phi + 2i \gamma_1 \Gamma_{12} \gamma_2 \sin \phi)}{2\Gamma_{12} (\Gamma_1 + i \Delta_1) \chi}, \quad (28)$$

$$\alpha_{21} = \frac{g_1 g_2 r_a \sqrt{1 - \eta^2} (\chi \cos \phi - 2i \gamma_2 \Gamma_{12} \gamma_1 \sin \phi)}{2\Gamma_{12} (\Gamma_2 + i \Delta_2) \chi}, \quad (29)$$

$$\alpha_{22} = \frac{g_2^2 r_a \Gamma_{12} \gamma_1 (1 - \eta)}{(\Gamma_2 + i \Delta_2) \chi}. \quad (30)$$

It is worth noting that when atoms are pumped into the cavity in state $|a_1\rangle$ or $|a_2\rangle$ (i.e., when $\eta = \pm 1$) the off-diagonal terms α_{12} and α_{21} vanish. This implies that the cross-correlation terms in the master equation disappear, which results in disentanglement of the cavity modes.

1. Transient regime

Since the HZ criterion involves fourth-order correlation and many coupled differential equations, obtaining analytical solutions is an involved problem. We thus present the results of our numerical simulations. We begin by investigating the dependence of the entanglement on the detuning. Figure 2(a) illustrates the HZ criterion as a function of dimensionless time $\gamma_2 t$ for various values of detunings Δ_1 and Δ_2 . Here other parameters are chosen so as to comply with the micromaser experiments [21,22]. We assume that the cavity modes are initially in a product state (cavity mode 1 in a number state with 5 photons and cavity mode 2 in a vacuum state, i.e., $|\Psi(0)\rangle_F = |5_1 0_2\rangle$) and atoms are injected into the cavity in a state $|\Psi(0)\rangle_A = \frac{1}{2}(|a_1\rangle + |a_2\rangle)$ or $\eta = 0$. As can be seen from Fig. 2(a), the quantity E_{HZ} is negative for short time for all cases indicating creation of entanglement between the cavity modes. We also observe that the transient entanglement vanishes at longer time scale for identical detunings $\Delta_1 = \Delta_2 = 80\gamma_2$. However, steady-state entanglement is achieved when the cavity detunings are different. This is quite interesting and markedly different from the result reported when one induces the coherence via a strong laser field [4–6]. We thus note that in order to create a steady-state entanglement, which is more applicable for a quantum information processing schemes, one should induce coherence between atomic levels before

injecting atoms into the cavity and by setting the cavity modes at different detunings.

Next we explore how the initial populations and coherences influence the entanglement dynamics. Figure 2(b) shows the plot of the quantity E_{HZ} versus $\gamma_2 t$ for fixed detunings ($\Delta_1 = 20\gamma_2$ and $\Delta_2 = 80\gamma_2$) and for various values of η . Recall that $\eta = \pm 1$ corresponds to no coherence whereas other values of η gives nonzero coherence. Figure 2(b) reveals that whenever there is coherence, the system exhibit transient as well as steady-state entanglement. Moreover, as the coherence decreases from maximum value $\eta = 0$ to no coherence $\eta = -1$, the value of the quantity E_{HZ} approaches to zero faster. That means, for weak coherence, the generated entanglement is more susceptible to dephasing processes.

So far we have assumed no dephasing in the system, that is, that the dephasing rate is the same as the spontaneous emission rate $\Gamma = \gamma_2$. However, the dephasing rates are in general higher than the spontaneous emission and cavity decay rates and may alter the entanglement behavior substantially. The dephasing rates Γ_1 and Γ_2 corresponding to the single-photon lasing transitions $|a_1\rangle \leftrightarrow |b\rangle$ and $|a_2\rangle \leftrightarrow |b\rangle$ are in general smaller than the two-photon dephasing rate Γ_{12} . However, for the sake of simplicity, we assume all dephasing rates to be the same, $\Gamma = \Gamma_{12} = \Gamma_1 = \Gamma_2$. Now, keeping the initial atomic coherence at maximum value ($\eta = 0$), we explore the effect of dephasing on the dynamics of the entanglement in the system. Figure 2(c) shows the plots of the quantity E_{HZ} versus $\gamma_2 t$ for $\Delta_1 = 20\gamma_2$, $\Delta_2 = 80\gamma_2$ for various quantity of dephasing rate. This figure indicates that the entanglement is sensitive to dephasing. For instance, when the dephasing rate is increased to $\Gamma = 4\gamma_2$, only the transient entanglement survives. When one further increases the dephasing rate to $\Gamma = 5\gamma_2$ the entanglement disappears. To keep the entanglement intact even in the presence of dephasing one can, in principle, tune other system parameters. To produce a robust steady-state entanglement one has to choose a parameter range for which the system operates in a large detuning condition. In Fig. 3, we plot the quantity E_{HZ} versus $\gamma_2 t$ for $g_1 = 5\gamma_2$, $g_2 = 2.15\gamma_2$, $\Gamma = \Gamma_{12} = \Gamma_1 = \Gamma_2 = 5\gamma_2$, $\gamma_1 = 1.25\gamma_2$, $\Delta_1 = 500\gamma_2$, $\Delta_2 = 100\gamma_2$, $\eta = 0$, and various values of pumping rate r_a . As can be seen from this figure, for $r_a = 1.1\gamma_2$ the quantity E_{HZ} is always positive, indicating no entanglement. However, if one gradually increases the

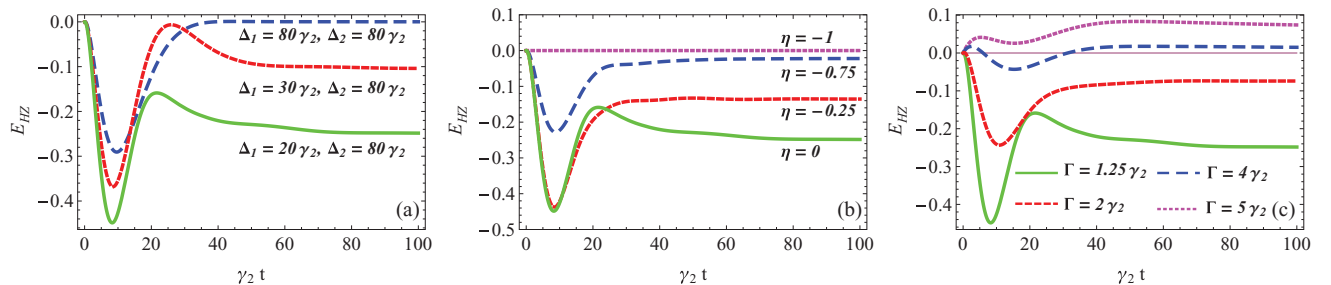


FIG. 2. (Color online) Plots of HZ criterion vs $\gamma_2 t$ for $g_1 = 50$ kHz, $g_2 = 43$ kHz, $r_a = 22$ kHz, $\gamma_1 = 25$ kHz, $\gamma_2 = 20$ kHz, $\kappa_1 = 1.5$ kHz, and $\kappa_2 = 2$ kHz, with $\Gamma_{12} = \Gamma_1 = \Gamma_2 = \gamma_1$ (no dephasing condition), $\phi = \pi/2$ in the absence of the driving field ($\Omega = 0$) and when cavity mode 1 is initially in number state with 5 photons and mode 2 in a vacuum state: (a) $\eta = 0$ (maximum injected coherence) and various values of detunings, (b) $\Delta_1 = 20\gamma_2$, $\Delta_2 = 80\gamma_2$, and various initial conditions for the atoms (various values of η), and (c) $\Delta_1 = 20\gamma_2$, $\Delta_2 = 80\gamma_2$, $\eta = 0$, and various values of dephasing rates $\Gamma \equiv \Gamma_1 = \Gamma_2 = \Gamma_{12}$.

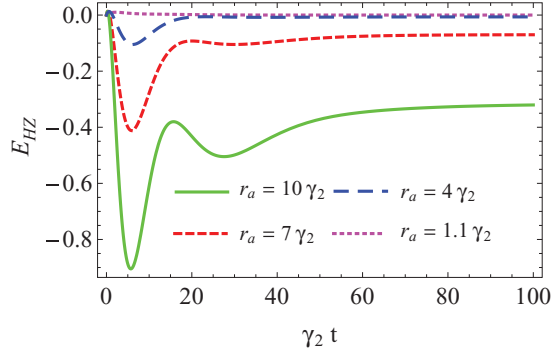


FIG. 3. (Color online) Plots of HZ criterion for $g_1 = 5\gamma_2$, $g_2 = 2.15\gamma_2$, $\gamma_1 = 1.25\gamma_2$, $\Gamma_{12} = \Gamma_1 = \Gamma_2 = 5\gamma_2$, $\Delta_1 = 500\gamma_2$, $\Delta_2 = 100\gamma_2$, $\kappa_1 = 0.2\gamma_2$, $\kappa_2 = 0.075\gamma_2$, $\eta = 0$, $\phi = \pi/2$, $\gamma_2 = 20$ kHz, in the absence of the driving field ($\Omega = 0$) and for various values of the pumping rate r_a . The initial condition for the cavity field is the same as in Fig. 2.

pumping rate, the system starts to exhibit transient entanglement for short times. Steady-state entanglement can also be achieved by further increasing the pumping rate of the atoms into the cavity. It is noteworthy to mention here that since the pumping rate is externally controllable, it is experimentally feasible to control the effect of dephasing on the entanglement at least for dephasing rates as high as $\Gamma = 5\gamma_2$. In essence, the adverse effect of dephasing can be counterbalanced by tuning the pumping rate accordingly.

2. Steady-state regime

As pointed out earlier, the cavity modes exhibit steady-state entanglement. We here explore the entanglement as a function of system parameters and effect of dephasing. An analytical solution for this case is also nontrivial; we thus solve the coupled equations and evaluate the function E_{HZ} numerically. In order to see the entanglement behavior as a function of the initial coherence, we then plot the quantity E_{HZ} as a function of η (see Fig. 4). It is easy to see from this figure that the system exhibits steady-state entanglement for all values of η except $\eta = \pm 1$, which confirms our previous assertion. We also observe that the entanglement exists only when the two cavity detunings are different. For example, for $\Delta_1 = \Delta_2 = 80\gamma_2$, the entanglement vanishes. Besides, it is counterintuitive

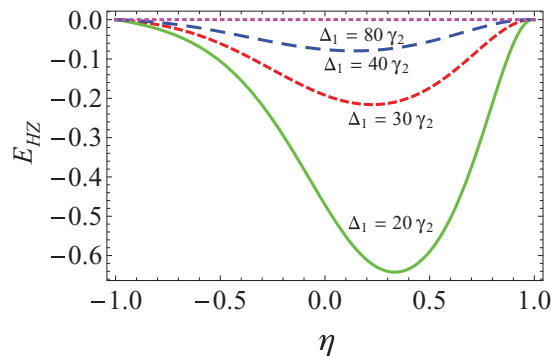


FIG. 4. (Color online) Plots of HZ criterion in the steady state vs η for $\Delta_2 = 80\gamma_2$ and for various values of Δ_1 . All other parameters as the same as in Fig. 2.

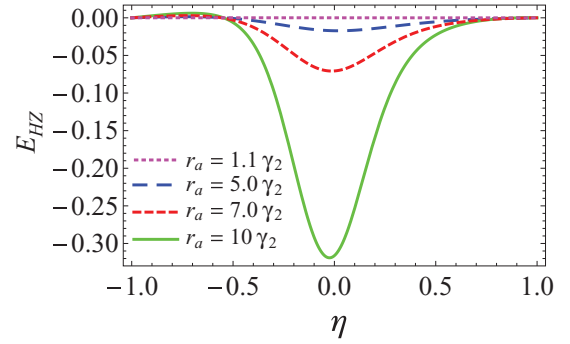


FIG. 5. (Color online) Plots of HZ criterion in the steady state vs η for dephasing rate $\Gamma = 5\gamma_2$ and for various values of pumping rates. All other parameters as the same as in Fig. 3.

to see that the minima for the E_{HZ} function does not occur at maximum initial coherence, $\eta = 0$. They rather appear for values of η between 0 and 0.5, depending on the value of the detuning Δ_1 . This shows that for this range of detunings, robust steady-state entanglement can be obtained by initially injecting more atoms in level $|a_2\rangle$ than $|a_1\rangle$.

To clearly see the effect of dephasing on steady-state entanglement, we plot in Fig. 5 the HZ criterion as a function of η for dephasing rate $\Gamma = 5\gamma_2$, and $\Delta_1 = 500\gamma_2$, $\Delta_2 = 100\gamma_2$, and other parameters are the same as in Fig. 3. As can be seen from this figure, by increasing the pumping rates, one can counterbalance the dephasing effect. However, this works only for the strong coherence condition, that is, when $\eta \approx [-0.5, 0.5]$. We also note that the entanglement is relatively robust at maximum coherence $\eta = 0$. We thus observe that when the system is far detuned and at higher pumping rates only strong initial coherence can create entanglement.

B. Entanglement via driven coherence

In this section, the role of dephasing on entanglement dynamics when the atomic coherence is induced by coupling of the upper two levels by an external laser is investigated. We assume that atoms are injected in their excited state $|a_1\rangle$, that is, no coherence at the initial time. The evolution of entanglement in a quantum-beat laser when coherence is induced by a strong laser field has been previously considered without taking into account the dephasing processes [4–6]. Here we focus on how the generated entanglement is modified by the dephasing rate.

The master equation corresponding to driven coherence which is obtained by setting $\eta = -1$ in Eq. (24) reads

$$\begin{aligned} \dot{\rho} = & \beta_{11}^*(\hat{a}_1^\dagger \hat{\rho} \hat{a}_1 - \hat{a}_1 \hat{a}_1^\dagger \hat{\rho}) + \beta_{11}(\hat{a}_1^\dagger \hat{\rho} \hat{a}_1 - \hat{\rho} \hat{a}_1 \hat{a}_1^\dagger) \\ & + \beta_{22}^*(\hat{a}_2^\dagger \hat{\rho} \hat{a}_2 - \hat{a}_2 \hat{a}_2^\dagger \hat{\rho}) + \beta_{22}(\hat{a}_2^\dagger \hat{\rho} \hat{a}_2 - \hat{\rho} \hat{a}_2 \hat{a}_2^\dagger) \\ & + [\beta_{21}^*(\hat{a}_1^\dagger \hat{\rho} \hat{a}_2 - \hat{a}_1^\dagger \hat{a}_2 \hat{\rho}) + \beta_{12}(\hat{a}_1^\dagger \hat{\rho} \hat{a}_2 - \hat{\rho} \hat{a}_1^\dagger \hat{a}_2)] e^{-i\phi} \\ & + [\beta_{12}^*(\hat{a}_2^\dagger \hat{\rho} \hat{a}_1 - \hat{a}_2^\dagger \hat{a}_1 \hat{\rho}) + \beta_{21}(\hat{a}_2^\dagger \hat{\rho} \hat{a}_1 - \hat{\rho} \hat{a}_2^\dagger \hat{a}_1)] e^{i\phi} \\ & + \sum_{j=1}^2 \frac{\kappa_j}{2} (2\hat{a}_j \hat{\rho} \hat{a}_j^\dagger - \hat{a}_j^\dagger \hat{a}_j \hat{\rho} - \hat{\rho} \hat{a}_j^\dagger \hat{a}_j), \end{aligned} \quad (31)$$

where

$$\beta_{11} = \frac{2g_1^2 r_a}{\Upsilon} [4\gamma_2 \Gamma_{12} (\Gamma_2 + i\Delta_2) + (-\gamma_2 + 4\Gamma_2 + 4i\Delta_2) \Omega^2], \quad (32)$$

$$\beta_{12} = \frac{2ig_1 g_2 r_a}{\Upsilon} [\Omega^2 - 2\gamma_2 (\Gamma_2 + i\Delta_2)], \quad (33)$$

$$\beta_{21} = \frac{2ig_1 g_2 r_a}{\Upsilon} [\Omega^2 + 2\gamma_2 (\Gamma_1 + \Gamma_{12} + i\Delta_1)], \quad (34)$$

$$\beta_{22} = \frac{2g_2^2 r_a}{\Upsilon} (2\Gamma_1 + \gamma_2 + 2i\Delta_1) \Omega^2, \quad (35)$$

where

$$\Upsilon \equiv \chi [4(\Gamma_1 + i\Delta_1)(\Gamma_2 + i\Delta_2) + \Omega^2].$$

We note that this master equation has the same form as that of the injected coherence, but the interpretation is different. When the driving laser field is turned off ($\Omega = 0$), the cross terms do not vanish. However, a close inspection of Eq. (35) shows that when we turn off the driving laser field, the gain for mode a_2 vanishes. This implies that population transfer from the initially populated level $|a_1\rangle$ to level $|a_2\rangle$ will not occur and hence no buildup of coherence between these two levels. As analytical solutions are rather nontrivial, we only present numerical results.

We consider an initial condition for the cavity field to be $|25_1 0_2\rangle$. In Fig. 6, we plot the HZ entanglement criterion versus dimensionless time $\gamma_2 t$ when the cavity modes are tuned with their respective atomic transitions and for various values of the Rabi frequency of the laser field. This figure shows that an initial product state evolves to an entangled state even in the presence of cavity losses [4]. However, the time of entanglement is limited by the strength of the applied driving laser. This can be understood by recalling that the coherence, which is responsible for the creation of entanglement in this model, strongly relies on the strength of laser field. For this reason, the existence of entanglement crucially depends on the field strength.

Furthermore, a natural question that follows is how this transient entanglement behaves in the presence of dephasing. In Fig. 7, we present the effect of dephasing on dynamical

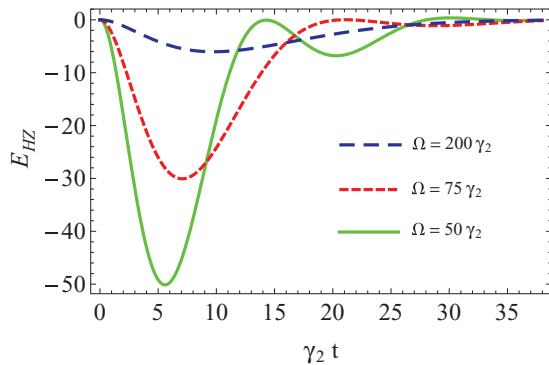


FIG. 6. (Color online) Temporal behavior of HZ criterion when the cavity modes are initially in a product state $|\Psi(0)\rangle = |25_1 0_2\rangle$ and when atoms are injected in their excited state $|a_1\rangle$ and for $\Delta_1 = \Delta_2 = 0$, $\Gamma = \gamma_2$. The curves correspond to various values of Rabi frequencies. All other parameters are the same as in Fig. 2(a).

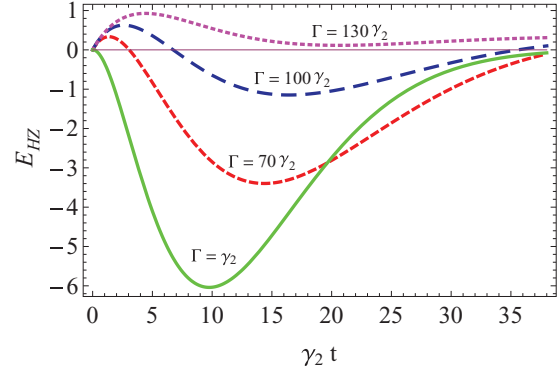


FIG. 7. (Color online) Temporal behavior of HZ criterion for laser field of Rabi frequency $\Omega = 200\gamma_2$. The curves correspond to various values of dephasing rates. All other parameters are the same as in Fig. 6.

behavior of entanglement for $\Omega = 200\gamma_2$, $\Delta_1 = \Delta_2 = 0$, and for various values of the dephasing rate Γ . It is worth noting that the requirement of nonzero detuning for having a well-behaved solution is now lifted due to the presence of a strong laser field. As illustrated in Fig. 7, in the presence of dephasing, the initial product state gets entangled after a short time. However, when the dephasing rate increases, the two cavity modes remain unentangled for sometime and get entangled for a longer window of time before they become disentangled again. In addition, the time for which the modes remain entangled gets shorter with increasing dephasing rate. For the parameters given in Fig. 7, the transient entanglement eventually vanishes when the dephasing rate becomes more than two orders of magnitude stronger than the spontaneous emission rate. Further, comparison of Figs. 3 and 7 shows that the entanglement generated via driven coherence is more robust against dephasing than that created via injected coherence. This might be explained in terms of the nature of the coherence induced by the two methods. It is clear that the coherence induced by the driving laser field is strong and controllable while the injected coherence is rather weak and fixed once the atoms are pumped into the cavity.

IV. CONCLUSION

We have studied the effect of dephasing on the entanglement generated in a quantum-beat laser via quantum coherence induced either by initially injected atoms in a coherent superposition of atomic levels or coupling the same levels by strong laser field. It turns out that the injected coherence give rise to transient as well as steady-state entanglement for realistic parameters. The steady-state entanglement exists only when the cavity detunings are different and relies strongly on the detunings and pumping rates. Moreover, the entanglement is more sensitive to dephasing processes. We show that the adverse effect of dephasing on the entanglement can be circumvented by injecting atoms into the cavity at higher pumping rates. On the other hand, it appears that the entanglement created through coherence induced by coupling of atomic levels by a strong laser field is relatively robust against dephasing. The formulation outlined in this work

provides a way to analyze the inevitable effect of dephasing processes on quantum features exhibited by two-photon lasers.

ACKNOWLEDGMENTS

The author thanks Konstantin E. Dorfman for helpful discussions and is supported by the Herman F. Heep and Minnie Belle Heep Texas A&M University Endowed Fund held and administered by the Texas A&M Foundation.

APPENDIX A: COEFFICIENTS IN THE MASTER EQUATION EQ. (24)

The coefficients that appear in the master equation (24) are

$$\begin{aligned} \zeta_{11} = & \frac{g_1^2 r_a}{\mathcal{D}} \{ \Gamma_{12} [4\gamma_2 \Gamma_{12} (\Gamma_2 + i\Delta_2) (1 - \eta) \\ & + [\gamma_1 - \gamma_2 + 4\Gamma_2 + 4i\Delta_2 + (\gamma_1 + \gamma_2)\eta] \Omega^2 \\ & + \Omega \sqrt{1 - \eta^2} [i\chi \cos \phi + 2\gamma_2 \Gamma_{12} (\gamma_1 + 2\Gamma_2 \\ & + 2i\Delta_2) \sin \phi] \}, \end{aligned} \quad (\text{A1})$$

$$\begin{aligned} \zeta_{12} = & \frac{2g_1 g_2 r_a}{\mathcal{D}} \{ i\Gamma_{12} \Omega [-\gamma_2 (\Gamma_2 + i\Delta_2) (1 - \eta) \\ & + \gamma_1 (\Gamma_2 + \Gamma_{12} + i\Delta_2) (1 + \eta) + \Omega^2] \\ & + \sqrt{1 - \eta^2} [(\Gamma_2 + i\Delta_2) \chi \cos \phi \\ & + i\gamma_1 \Gamma_{12} (2\gamma_2 \Gamma_2 + 2i\gamma_2 \Delta_2 - \Omega^2) \sin \phi] \}, \end{aligned} \quad (\text{A2})$$

$$\begin{aligned} \zeta_{21} = & \frac{2g_1 g_2 r_a}{\mathcal{D}} \{ i\Gamma_{12} \Omega [-\gamma_1 (\Gamma_1 + i\Delta_1) (1 + \eta) \\ & + \gamma_2 (\Gamma_1 + \Gamma_{12} + i\Delta_1) (1 - \eta) + \Omega^2] \\ & + \sqrt{1 - \eta^2} [(\Gamma_1 + i\Delta_1) \chi \cos \phi \\ & - i\gamma_2 \Gamma_{12} (2\gamma_1 \Gamma_1 + 2i\gamma_1 \Delta_1 - \Omega^2) \sin \phi] \}, \end{aligned} \quad (\text{A3})$$

$$\begin{aligned} \zeta_{22} = & \frac{g_2^2 r_a}{\mathcal{D}} \{ \Gamma_{12} [4\gamma_1 \Gamma_{12} (\Gamma_1 + i\Delta_1) (1 + \eta) \\ & + [\gamma_2 - \gamma_1 + 4\Gamma_1 + 4i\Delta_1 - (\gamma_1 + \gamma_2)\eta] \Omega^2 \\ & + \Omega \sqrt{1 - \eta^2} [i\chi \cos \phi - 2\gamma_1 \Gamma_{12} (\gamma_2 + 2\Gamma_1 \\ & + 2i\Delta_1) \sin \phi] \}, \end{aligned} \quad (\text{A4})$$

where

$$\mathcal{D} = \Gamma_{12} \chi [4(\Gamma_1 + i\Delta_1)(\Gamma_2 + i\Delta_2) + \Omega^2], \quad (\text{A5})$$

$$\chi = 2\gamma_1 \gamma_2 \Gamma_{12} + (\gamma_1 + \gamma_2) \Omega^2. \quad (\text{A6})$$

APPENDIX B: EQUATIONS OF EVOLUTION FOR EXPECTATION VALUES OF CAVITY MODE VARIABLES

Using the master equation derived in Sec. II, we derive the equations of evolution for the expectation values of the cavity mode operators. In general, the evolution of the expectation value of an operator can be written as $d\langle \hat{\rho} \rangle / dt = \text{Tr}(\hat{\rho} \frac{d\hat{\rho}}{dt})$. By applying this together with the master equation given by (24), we obtain

$$\frac{d}{dt} \langle \hat{a}_1^2 \rangle = (2\zeta_{11} - \kappa_1) \langle \hat{a}_1^2 \rangle + 2\zeta_{12} \langle \hat{a}_1 \hat{a}_2 \rangle e^{-i\phi}, \quad (\text{B1})$$

$$\frac{d}{dt} \langle \hat{a}_2^2 \rangle = (2\zeta_{22} - \kappa_2) \langle \hat{a}_2^2 \rangle + 2\zeta_{21} \langle \hat{a}_1 \hat{a}_2 \rangle e^{i\phi}, \quad (\text{B2})$$

$$\begin{aligned} \frac{d}{dt} \langle \hat{a}_1 \hat{a}_2 \rangle = & [\zeta_{11} + \zeta_{22} - \frac{1}{2}(\kappa_1 + \kappa_2)] \langle \hat{a}_1 \hat{a}_2 \rangle + \zeta_{21} \langle \hat{a}_1^2 \rangle e^{i\phi} \\ & + \zeta_{12} \langle \hat{a}_2^2 \rangle e^{-i\phi}, \end{aligned} \quad (\text{B3})$$

$$\begin{aligned} \frac{d}{dt} \langle \hat{a}_1^\dagger \hat{a}_1 \rangle = & (\zeta_{11} + \zeta_{11}^* - \kappa_1) \langle \hat{a}_1^\dagger \hat{a}_1 \rangle + \zeta_{12} \langle \hat{a}_1^\dagger \hat{a}_2 \rangle e^{-i\phi} \\ & + \zeta_{12}^* \langle \hat{a}_1 \hat{a}_2^\dagger \rangle e^{i\phi} + \zeta_{11} + \zeta_{11}^*, \end{aligned} \quad (\text{B4})$$

$$\begin{aligned} \frac{d}{dt} \langle \hat{a}_2^\dagger \hat{a}_2 \rangle = & (\zeta_{22} + \zeta_{22}^* - \kappa_2) \langle \hat{a}_2^\dagger \hat{a}_2 \rangle + \zeta_{21} \langle \hat{a}_2^\dagger \hat{a}_1 \rangle e^{i\phi} \\ & + \zeta_{21}^* \langle \hat{a}_2 \hat{a}_1^\dagger \rangle e^{-i\phi} + \zeta_{22} + \zeta_{22}^*, \end{aligned} \quad (\text{B5})$$

$$\begin{aligned} \frac{d}{dt} \langle \hat{a}_1^\dagger \hat{a}_2 \rangle = & [\zeta_{11}^* + \zeta_{22} - \frac{1}{2}(\kappa_1 + \kappa_2)] \langle \hat{a}_1^\dagger \hat{a}_2 \rangle + \zeta_{21} \langle \hat{a}_1^\dagger \hat{a}_1 \rangle e^{i\phi} \\ & + \zeta_{12}^* \langle \hat{a}_2^\dagger \hat{a}_2 \rangle e^{i\phi} + (\zeta_{21} + \zeta_{12}^*) e^{i\phi}, \end{aligned} \quad (\text{B6})$$

$$\begin{aligned} \frac{d}{dt} \langle n_1 n_2 \rangle = & (\zeta_{11} + \zeta_{11}^* + \zeta_{22} + \zeta_{22}^* - \kappa_1 - \kappa_2) \langle n_1 n_2 \rangle \\ & + [\zeta_{12}^* \langle \hat{a}_1 \hat{a}_2^{\dagger 2} \hat{a}_2 \rangle + \zeta_{21} \langle \hat{a}_1^\dagger \hat{a}_1^2 \hat{a}_1^\dagger \rangle + (\zeta_{12}^* + \zeta_{21}) \\ & \times \langle \hat{a}_1 \hat{a}_2^\dagger \rangle] e^{i\phi} + [\zeta_{21}^* \langle \hat{a}_1^{\dagger 2} \hat{a}_1 \hat{a}_2 \rangle + \zeta_{12} \langle \hat{a}_2^\dagger \hat{a}_2^2 \hat{a}_1^\dagger \rangle \\ & + (\zeta_{21}^* + \zeta_{12}) \langle \hat{a}_1^\dagger \hat{a}_2 \rangle] e^{-i\phi} + (\zeta_{11}^* + \zeta_{11}) \langle \hat{a}_2^\dagger \hat{a}_2 \rangle \\ & + (\zeta_{22}^* + \zeta_{22}) \langle \hat{a}_1^\dagger \hat{a}_1 \rangle, \end{aligned} \quad (\text{B7})$$

$$\begin{aligned} \frac{d}{dt} \langle \hat{a}_1 \hat{a}_2^{\dagger 2} \hat{a}_2 \rangle = & [\zeta_{11} + \zeta_{22} + 2\zeta_{22}^* - \frac{1}{2}(\kappa_1 + 3\kappa_2)] \langle \hat{a}_1 \hat{a}_2^{\dagger 2} \hat{a}_2 \rangle \\ & + \zeta_{21} \langle \hat{a}_1^2 \hat{a}_2^{\dagger 2} \rangle e^{i\phi} + [\zeta_{12} \langle \hat{a}_2^{\dagger 2} \hat{a}_2 \rangle \\ & + 2(\zeta_{12} + \zeta_{21}^*) \langle \hat{a}_2^\dagger \hat{a}_2 \rangle + 2\zeta_{21}^* \langle n_1 n_2 \rangle] e^{-i\phi} \\ & + 2(\zeta_{22} + \zeta_{22}^*) \langle \hat{a}_1 \hat{a}_2^\dagger \rangle, \end{aligned} \quad (\text{B8})$$

$$\begin{aligned} \frac{d}{dt} \langle \hat{a}_1^\dagger \hat{a}_1^2 \hat{a}_2^\dagger \rangle = & [\zeta_{11}^* + 2\zeta_{11} + \zeta_{22}^* - \frac{1}{2}(3\kappa_1 + \kappa_2)] \langle \hat{a}_1^\dagger \hat{a}_1^2 \hat{a}_2^\dagger \rangle \\ & + \zeta_{12}^* \langle \hat{a}_1^2 \hat{a}_2^{\dagger 2} \rangle e^{i\phi} + [\zeta_{21}^* \langle \hat{a}_1^{\dagger 2} \hat{a}_1 \rangle \\ & + 2(\zeta_{12} + \zeta_{21}^*) \langle \hat{a}_1^\dagger \hat{a}_1 \rangle + 2\zeta_{12} \langle n_1 n_2 \rangle] e^{-i\phi} \\ & + 2(\zeta_{11} + \zeta_{11}^*) \langle \hat{a}_1 \hat{a}_2^\dagger \rangle, \end{aligned} \quad (\text{B9})$$

$$\begin{aligned} \frac{d}{dt} \langle \hat{a}_2^2 \hat{a}_2^{\dagger 2} \rangle = & 2[\zeta_{11} + \zeta_{22}^* - \frac{1}{2}(\kappa_1 + \kappa_2)] \langle \hat{a}_1^2 \hat{a}_2^{\dagger 2} \rangle \\ & + [2\zeta_{21}^* \langle \hat{a}_1^\dagger \hat{a}_2^2 \hat{a}_1^\dagger \rangle + 2\zeta_{12} \langle \hat{a}_2^{\dagger 2} \hat{a}_2 \hat{a}_1 \rangle \\ & + 4(\zeta_{21}^* + \zeta_{12}) \langle \hat{a}_1 \hat{a}_2^\dagger \rangle] e^{-i\phi}, \end{aligned} \quad (\text{B10})$$

$$\begin{aligned} \frac{d}{dt} \langle \hat{a}_1^{\dagger 2} \hat{a}_1^2 \rangle = & 2(\zeta_{11} + \zeta_{11}^* - \kappa_1) \langle \hat{a}_1^{\dagger 2} \hat{a}_1^2 \rangle + 2\zeta_{12}^* \langle \hat{a}_1^\dagger \hat{a}_2^2 \hat{a}_1^\dagger \rangle e^{i\phi} \\ & + 2\zeta_{12} \langle \hat{a}_1^{\dagger 2} \hat{a}_1 \hat{a}_2 \rangle e^{-i\phi} + 4(\zeta_{11}^* + \zeta_{11}) \langle \hat{a}_1^\dagger \hat{a}_1 \rangle, \end{aligned} \quad (\text{B11})$$

$$\begin{aligned} \frac{d}{dt} \langle \hat{a}_2^{\dagger 2} \hat{a}_2^2 \rangle = & 2(\zeta_{22} + \zeta_{22}^* - \kappa_2) \langle \hat{a}_2^{\dagger 2} \hat{a}_2^2 \rangle + 2\zeta_{21} \langle \hat{a}_1 \hat{a}_2^{\dagger 2} \hat{a}_2 \rangle e^{i\phi} \\ & + 2\zeta_{21}^* \langle \hat{a}_2^{\dagger 2} \hat{a}_2 \hat{a}_1^\dagger \rangle e^{-i\phi} + 4(\zeta_{22}^* + \zeta_{22}) \langle \hat{a}_2^\dagger \hat{a}_2 \rangle. \end{aligned} \quad (\text{B12})$$

- [1] H. Xiong, M. O. Scully, and M. S. Zubairy, *Phys. Rev. Lett.* **94**, 023601 (2005).
- [2] E. Alebachew, *Phys. Rev. A* **76**, 023808 (2007); E. A. Sete, *Opt. Commun.* **281**, 6124 (2008).
- [3] E. Alebachew, *Opt. Commun.* **280**, 133 (2007).
- [4] S. Qamar, F. Ghafoor, M. Hillery, and M. S. Zubairy, *Phys. Rev. A* **77**, 062308 (2008).
- [5] A. P. Fang, Y. L. Chen, F. L. Li, H. R. Li, and P. Zhang, *Phys. Rev. A* **81**, 012323 (2010).
- [6] R. Tahira, M. Ikram, H. Nha, and M. S. Zubairy, *Phys. Rev. A* **83**, 054304 (2011).
- [7] E. A. Sete, K. E. Dorfman, and J. P. Dowling, *J. Phys. B* **44**, 225504 (2011).
- [8] W. Bickel and S. Bashkin, *Phys. Rev.* **162**, 12 (1967).
- [9] W. Chow, M. Scully, and J. Stoner, *Phys. Rev. A* **11**, 1380 (1975).
- [10] R. Herman, H. Grotch, R. Kornblith, and J. Eberly, *Phys. Rev. A* **11**, 1389 (1975).
- [11] M. O. Scully, *Phys. Rev. Lett.* **55**, 2802 (1985).
- [12] M. O. Scully and M. S. Zubairy, *Phys. Rev. A* **35**, 752 (1987).
- [13] O. Kocharovskaya and Ya. I. Khanin, *JETP Lett.* **48**, 630 (1988); S. E. Harris, *Phys. Rev. Lett.* **62**, 1033 (1989); M. O. Scully, S. Y. Zhu, and A. Gavrielides, *ibid.* **62**, 2813 (1989).
- [14] M. Hillery and M. S. Zubairy, *Phys. Rev. A* **74**, 032333 (2006).
- [15] W. H. Louisell, *Quantum Statistical Properties of Radiation* (Wiley, New York, 1973).
- [16] M. O. Scully and M. S. Zubairy, *Quantum Optics* (Cambridge University Press, Cambridge, UK, 1997).
- [17] F. Kassahun, *Fundamentals of Quantum Optics* (Lulu, Raleigh, NC, 2008).
- [18] The result of Eq. (4) can be obtained by applying a mathematical relation $\frac{d}{dx} \int_a^x f(x,y)dy = f(x,x) - f(x,a) + \int_a^x \frac{\partial}{\partial x} f(x,y)dy$ in Eq. (3).
- [19] G. S. Agarwal and A. Biswas, *New J. Phys.* **7**, 211 (2005).
- [20] H. Nha and J. Kim, *Phys. Rev. A* **74**, 012317 (2006).
- [21] D. Meschede, H. Walther, and G. Muller, *Phys. Rev. Lett.* **54**, 551 (1985).
- [22] J. M. Raimond, M. Brune, and S. Haroche, *Rev. Mod. Phys.* **73**, 565 (2001).